International Journal of Solids and Structures 75–76 (2015) 277–286

Contents lists available at ScienceDirect

International Journal of Solids and Structures

journal homepage: www.elsevier.com/locate/ijsolstr

Rate dependent fracture of a double cantilever beam with combined bulk and interfacial dissipation

Shawn R. Lavoie [a], Rong Long [a,b], Tian Tang [a,*]

[a] Department of Mechanical Engineering, 4-9 Mechanical Engineering Building, University of Alberta, Edmonton, AB T6G 2G8, Canada
[b] Department of Mechanical Engineering, University of Colorado at Boulder, Boulder, CO 80303, USA

ARTICLE INFO

Article history:
Received 12 March 2015
Received in revised form 22 July 2015
Available online 1 September 2015

Keywords:
Viscoelasticity
Rate dependent bond rupture
Adhesion
Double cantilever beam
Fracture energy
Viscous dissipation

ABSTRACT

The energy required to fracture viscoelastic media is known to depend on the rate of crack propagation. In this work, crack propagation, driven by applied moments, in an idealized model of a viscoelastic double cantilever beam (DCB) is studied. Rate dependency is taken into account through a standard linear solid viscoelastic model for the bulk material, and an adhesive zone model describing bond rupture kinetics for the polymer chains which bridge the interface. Attractive van der Waals (*vdW*) forces are also taken into account within the adhesive zone. The apparent energy release rate consists of two parts: the energy to overcome adhesion on the interface as well as viscous dissipation in the bulk. The adhesive energy in rupturing polymer chains increases as crack propagation speed increases. Relaxation of the bulk material causes viscous dissipation as stored strain energy is lost. For a beam of fixed length this dissipation was found to be negligible at high and low rates of crack propagation. Between these two limits there is a critical crack propagation speed where viscous dissipation is maximized.

1. Introduction

The failure of polymeric materials is a phenomenon frequently encountered in a wide range of technological applications. Many of these materials display viscoelastic properties upon mechanical loading. However, the fracture mechanics of viscoelastic materials has yet to be fully understood (Gent 1996). Numerous experimental studies have found that the energy required to fracture polymeric materials depends on the rate of fracture (Lake and Thomas 1967; Gent 1996; Chaudhury 1999; Ghatak et al. 2000). The work needed to propagate a crack at constant speed is often found to increase as the speed is increased (Gent 1996; Hui et al. 2004). A similar phenomenon has also been observed for viscoelastic adhesives. Gent and Schultz found that the energy needed to peel viscoelastic rubbery adhesives was strongly dependent on the rate of peeling (Gent and Shultz 1972; Kovalchick et al. 2014) had similar findings. The adhesive failure of amorphous rubber adhered to a rigid substrate was studied by Andrews and Kinloch (1973) who found that the energy required to detach the rubber consisted of two components: the intrinsic failure energy and the energy dissipated viscoelastically. Their results when reduced to a reference temperature using the Williams–Landel–Ferry (WLF) equation (Williams et al. 1955) yielded a single master curve, reminiscent of the time–temperature superposition for the relaxation modulus of viscoelastic materials. It is generally accepted that the energy supplied to propagate a crack at a constant speed must be sufficient to overcome energy dissipation in the bulk polymer (Xu et al. 1992; Gent 1996; Christiansen 2003) as well as the adhesive or cohesive energy on the crack interface (Xu et al. 1992; Chaudhury 1999; Ghatak et al. 2000; Hui et al. 2004), henceforth referred to as the fracture energy.

Several theoretical efforts have been made to quantify viscous dissipation in the bulk material. Xu et al. (1992) and Hui et al. (1992) studied the peeling of a viscoelastic double cantilever beam (DCB) as well as an infinite viscoelastic solid with small scale yielding. In both cases the viscoelastic material was modeled as a standard linear solid (Hui et al. 1992; Xu et al. 1992). Chen et al. (2013) and Gao and Su (2015) studied peeling of viscoelastic Bernouli-Euler beams using linear viscoelastic models which use the Boltzmann superposition integral. More sophisticated models which consider microstructural changes brought about by scission and reforming of polymer networks have been proposed (Rajagopal and Wineman 1992; Wineman 2009). These models can provide a more accurate description of viscoelastic polymers, especially under finite deformation, but would also add significant complexity to the problem.

* Corresponding author. Tel.: +1 780 492 5467; fax: +1 780 492 2200.
E-mail address: tian.tang@ualberta.ca (T. Tang).

http://dx.doi.org/10.1016/j.ijsolstr.2015.08.020
0020-7683/

There have also been works seeking to model interfacial phenomena for crack propagation in polymeric materials. Xu et al. (1992) and Hui et al. (1992) used a simple Dugdale-Barenblatt cohesive zone model with a constant cohesive stress, and a Newtonian fluid model with a cut-off stress to describe the cohesive interaction in their works. Lake and Thomas studied the failure of vulcanized rubber and concluded that the fracture energy was amplified by the number of monomer units on the chains bridging the crack (Lake and Thomas 1967). However, the Lake-Thomas theory did not explain why the fracture energy is rate dependent, and Chaudhury (1999) proposed that this rate dependency is related to chemical kinetic processes at the interface. To quantify the kinetics of such interfacial processes, Chaudhury (1999) introduced a kinetic equation, with the Lake and Thomas amplification factor incorporated, to study the dissociation of bonds bridging two interfaces as they were separated. This rate equation was later applied to a crack with an idealized wedge-shaped opening profile (Ghatak et al. 2000), and further to more realistic crack opening profiles (Hui et al. 2004). This approach differs from traditional rate-independent models where the criterion for interface separation is based on a critical energy release rate or cohesive stress. An overview of the historical application of chemical kinetics to interfacial problems and further justification for the use of kinetic equations in fracture problems was given by Chaudhury (1999).

The works cited above all made excellent contributions to advancing the field. However, in his review of several experiments, Gent (1996) concluded that rate dependency of the apparent energy release rate should result from a combined effect of both interfacial and bulk properties.

The conclusion that the interfacial model must also be rate dependent was reached by Rahulkumar et al. (2000) after attempting to match finite element results to experimental data for peel tests. Among the prior theoretical works several have considered basic bulk viscoelastic models (Hui et al. 1992; Xu et al. 1992), however the adhesive zone models used in these works were too simplistic. On the other hand, none of the prior works that captured rupture kinetics of the polymer chains bridging a crack have considered bulk viscoelastic behavior (Chaudhury 1999; Ghatak et al. 2000; Hui et al. 2004). The goal of this work is to develop a simple model which takes into account both bulk viscoelasticity and rate dependent rupture of polymer chains across the interface. We will accomplish this by considering steady state crack propagation in a simple viscoelastic DCB geometry which was used by (Xu et al. 1992). The crack will be reinforced by an adhesive zone with polymer chains which undergo rate dependent breakage following the kinetics previously presented in the literature (Chaudhury 1999; Ghatak et al. 2000; Hui et al. 2004).

The structure of the paper is as follows. The mathematical formulation of our model is presented in Section 2. The numerical methods used to solve the equations are described in Section 3. Numerical results are presented and discussed in Section 4. Conclusions are given in Section 5.

2. Formulation

The problem studied in this work is the rate dependent fracture of a viscoelastic material, represented by a DCB as shown in Fig. 1 (a). Here the applied moments M_∞ cause steady-state crack propagation at speed V, and separates the DCB into two identical beams. The rightmost point in the fully bonded portion (no separation) of the DCB is referred to as the adhesive zone tip. An adhesive zone is introduced to the right of the adhesive zone tip, within this zone stresses from both van der Waals (*vdW*) attractions and the stretch of polymer chains resist the separation of the two beams (see Fig. 1 (a)). As one moves away from the adhesive zone tip (to the right)

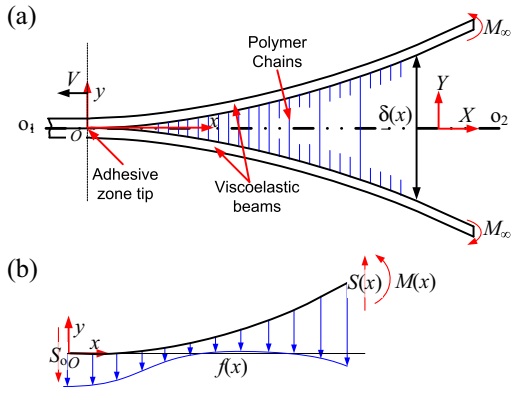

Fig. 1. (a) Schematic of the viscoelastic DCB studied in this work. The representative polymer chains shown in this figure are not meant to indicate the chains are disabled at some positions and enables at others. The density of chains is smaller for larger x. The crack-tip is the point where the bond density first becomes zero. (b) free body diagram of a section of the upper beam within the adhesive zone.

eventually stretched chains will rupture, which will reduce the density of chains bridging the crack tip and cause the adhesive stress to decrease. A suitable criterion will be specified later to define the crack tip as the leftmost point where these stresses vanish. The region between the adhesive zone tip and the crack tip is the adhesive zone. X–Y is a fixed coordinate system and x–y is a coordinate system which is attached to the adhesive zone tip and translates at constant speed V with the crack. The crack opening δ depends on position x. Because the two beams are assumed to be identical, the system is symmetrical about line o_1–o_2 which is the crack interface. Our goal is to calculate the energy required to propagate the crack at a given speed V. This energy consists of work required to overcome attractions in the adhesive zone, and energy dissipated by viscoelastic processes in the bulk material.

2.1. Viscoelastic Beam

Consider the free-body diagram of a section of the upper beam shown in Fig. 1(b). The beam is shown in a deflected state and is acted upon by a distributed adhesive stress f. f consists of contributions from polymer chains which bridge the crack interface and *vdW* attractions. An imaginary cut is made in the beam at x to reveal the two internal loads acting on the beam: a shear force S, and a bending moment M. At point O there is a reaction shear force S_o. Xu et al. (1992) formulated a differential equation for the deflection of a viscoelastic DCB:

$$M - \tau_o V S = \frac{E_\infty I}{2}\frac{d^2\delta}{dx^2} + \frac{\tau_o V E_o I}{2}\frac{d^3\delta}{dx^3}, \tag{1}$$

where I is the moment of inertia of the beams' cross section. The derivatives in the equation are with respect to x instead of time t because under steady state condition, the transformation $d/dt = V d/dx$ can be introduced using the translating coordinate system x–y fixed to the adhesive zone tip. Eq. (1) is based on a standard linear viscoelastic solid model, which for a uniaxial stress state reduces to the following stress–strain relation $\sigma + \tau_o\dot{\sigma} = E_\infty\varepsilon + \tau_o E_o\dot{\varepsilon}$, where E_o is the instantaneous or unrelaxed modulus, E_∞ is the infinite time or relaxed modulus, τ_o is the bulk relaxation time, σ is stress, ε is strain and the overhead dot $(\dot{\sigma}, \dot{\varepsilon})$ indicates differentiation with respect to time (Xu et al. 1992).

2.2. Rate Dependent Chain Rupture

The two beams are bridged by polymer chains. Kinetic equations can be written to model the rupture of bonds on the polymer chains; rupture of any one bond on a chain's backbone prevents it

from bridging the crack. When a tensile force (F) is applied to a chemical bond it decreases the activation energy of bond dissociation (Chaudhury 1999), and hence increases the probability of bond rupture. The number of chains bridging the two surfaces can be obtained from the solution of an equation governing the kinetics of bond rupture (Chaudhury 1999)

$$-V\frac{d\Sigma_b}{dx}=\frac{n}{\tau_-}\Sigma_b e^{F\lambda/k_BT}, \tag{2}$$

$$\Sigma_b(0)=\Sigma_o \tag{3}$$

In Eq. (2), Σ_b is the number of chains that cross a unit area of the interface, n is the number of bonds per polymer chain, λ is the bond activation length, F is the tensile force acting on each chain, k_B is the Boltzman constant, T is the absolute temperature and τ_- is the characteristic time of bond dissociation which depends on the activation energy for bond dissociation (Chaudhury 1999). In particular, $\tau_- = h_P e^{E_a/k_BT}/k_BT$, where h_p is Plank's constant; larger vibration energy of molecules at higher temperature allows more rapid passage over the activation energy (E_a) barrier and leads to faster dissociation. The right hand side of Eq. (2) is the rate of chain dissociation. Theoretically, there can also be a term responsible for chain association, but it is typically assumed to be considerably smaller than the chain dissociation rate and has been neglected (Chaudhury 1999). Eq. (2) is accompanied by a boundary condition Eq. (3) which states that at $x = 0$, where the crack opening is zero and the chains are not stretched, no chains are broken. Σ_o is the chain density for perfectly bonded interface. The original kinetic equation (Chaudhury 1999) is expressed in terms of the time derivative of Σ_b, which has been converted to a derivative with respect to position by using a steady-state assumption and a coordinate transformation ($d/dt = Vd/dx$) from the fixed X–Y system to the x–y system which translates with velocity V (see Fig. 1(a)). The tensile force acting on each chain, F, can be related to the extension of the polymer chains bridging the crack interface. Although the force-extension relationship is usually not linear (Ghatak et al. 2000), we will adopt an assumption from the literature where the chains are assumed to be linear springs (Chaudhury 1999; Hui et al. 2004), i.e., $F = k_s\delta$, where k_s is the average spring stiffness defined from $U=\int_0^{L_c} k_s\delta d\delta = k_s L_c^2/2$. Here U is the work required to stretch the chain from its unstressed configuration to its contour length L_c. Defining the average spring stiffness in this way ensures that the work U to stretch the linear chain is equal to that for its nonlinear counterpart.

The distributed load acting on the beams,

$$f=\Sigma_b F+\frac{W_{vdW}}{\delta_c}e^{-\delta/\delta_c}, \tag{4}$$

is made up of two components: the adhesive stress from polymer chains $\Sigma_b F$ (the force acting on each chain, F, times the density of chains Σ_b), and the attractive vdW stress $W_{vdW}e^{-\delta/\delta_c}/\delta_c$ where δ_c is a characteristic decay length and W_{vdW} is the work of adhesion due to vdW attractions. The inclusion of the vdW component of the adhesive stress was shown to be necessary in order to have a well-defined adhesive zone tip (Hui et al. 2004). This exponential function for vdW attractions is an approximation which has been chosen for mathematical convenience. It is well-known that dispersion forces decay much slower than the exponential function (Hui et al. 2004). However, provided that the vdW region is much smaller than the chain bridging region, it is expected, and demonstrated later in this work, that fracture problems are insensitive to the form of the vdW interaction potential as long as it produces the same work of adhesion (Hui et al. 2004).

2.3. Non-dimensionalized boundary value problem

The viscoelastic beam model introduced in Section 2.1 and the rate-dependent interface model described in Section 2.2 are combined to study the steady-state crack propagation in the DCB. The interface and beam models are coupled through the stretch of interfacial polymer chains and the resulting forces acting on the beams. Balance of the distributed load f on the interface with the internal shear forces S and moment M, shown in Fig. 1(b) (Hibbeler 2005), leads to a system of ordinary differential equations (ODEs) and boundary conditions (BCs). Through the formulation 16 parameters have been identified which define the rate of crack propagation, geometry and properties of the bulk and interfacial models: V, n, τ_-, λ, k_B, T, Σ_o, τ_o, E_o, E_∞, I, L_c, U, W_{vdW}, δ_c, and D. All of these parameters have been introduced in previous sections except the last one which is the out-of-plane depth of the beam. To reduce the number of parameters and simplify the ensuing discussion we introduce the following non-dimensional parameters.

$$\Sigma_b^*=\frac{\Sigma_b}{\Sigma_o},\quad x^*=x\left(\frac{2k_BT\Sigma_oD}{E_oIL_c^2}\right)^{1/4},\quad \delta^*=\frac{\delta}{L_c},\quad F^*=\frac{FL_c}{k_BT},$$
$$f^*=\frac{fL_c}{k_BT\Sigma_oD},\quad S^*=\frac{SL_c}{k_BT\Sigma_oD}\left(\frac{2k_BT\Sigma_oD}{E_oIL_c^2}\right)^{1/4},$$
$$M^*=M\left(\frac{2}{k_BT\Sigma_oDE_oI}\right)^{1/2},\quad V^*=\tau_oV\left(\frac{2k_BT\Sigma_oD}{E_oIL_c^2}\right)^{1/4},$$
$$U^*=\frac{U}{k_BT},\quad \gamma_E=\frac{E_\infty}{E_o},\quad \gamma_\tau=n\frac{\tau_o}{\tau_-},\quad \gamma_L=\frac{\lambda}{L_c},\quad \delta_c^*=\frac{\delta_c}{L_c},$$
$$W_{vdW}^*=\frac{W_{vdW}}{k_BT\Sigma_o},\quad G^*=\frac{G}{k_BT\Sigma_o},\quad G_{ad}^*=\frac{G_{ad}}{k_BT\Sigma_o},\quad G_{vis}^*=\frac{G_{vis}}{k_BT\Sigma_o}. \tag{5}$$

The physical meanings of the variables from Eq. (5) are summarized in Table 1.

After nondimensionalization using Eq. (5), the bond dissociation equation, Eqs. (2) and (3), becomes

$$\frac{d\Sigma_b^*}{dx^*}=-\frac{\gamma_\tau}{V^*}\Sigma_b^* e^{F^*\gamma_L}, \tag{6}$$

Table 1
Description of non-dimensional Parameters.

Category	Parameter	Description of non-dimensional parameter
Position-dependent variables	x^*	Position
	Σ_b^*	Bond density
	δ^*	Crack opening
	F^*	Force on a single polymer chain
	f^*	Distributed load on the interface
	S^*	Shear force
	M^*	Bending moment
Governing Parameters	V^*	Crack propagation speed
	U^*	Energy of a polymer chain when stretched to its full contour length
	γ_E	Ratio of relaxed to unrelaxed Young's modulus in the standard linear solid viscoelastic model
	γ_τ	Ratio of relaxation times of bulk and chain dissociation
	γ_L	Ratio of activation length to contour length
	δ_c^*	vdW decay length
	W_{vdW}^*	vdW work of adhesion
Fracture Energies (Desired Output)	G^*	Fracture energy
	G_{ad}^*	Adhesive fracture energy; describing interfacial dissipation
	G_{vis}^*	Viscous fracture energy; describing bulk dissipation

$$\Sigma_b^*(0) = 1, \tag{7}$$

and the polymer chain force-stretch relationship, becomes $F^* = 2U^*\delta^*$. Similarly, introduction of the parameters in Eq. (5) into the beam equation gives

$$M^* - V^*S^* = \gamma_E \frac{d^2\delta^*}{dx^{*2}} + V^* \frac{d^3\delta^*}{dx^{*3}}. \tag{8}$$

The balance of the shear force with the distributed load leads to

$$\frac{dS^*}{dx^*} = f^* = \Sigma_b^* F^* + \frac{W_{vdW}^*}{\delta_c^*} e^{-\delta^*/\delta_c^*}, \tag{9}$$

and the bending moment is related to the shear force by

$$\frac{dM^*}{dx^*} = -S^*. \tag{10}$$

Eqs. (8)–(10) contain two first order ODEs and one third order ODE, and should be accompanied by five BCs. Firstly, on the left of the adhesive zone at $x = 0$, the crack opening is identically zero therefore the slope and deflection at the adhesive zone tip will be zero or

$$\delta^*(0) = 0, \quad \frac{d\delta^*}{dx^*}(0) = 0. \tag{11}$$

Secondly, the steady-state assumption implies that the beams experience a sudden loading at the adhesive zone tip. As a result the material at the adhesive zone tip can be treated as elastic with the unrelaxed or instantaneous modulus. Using the j-integral (Rice 1968; Glassmaker and Hui 2004; Anderson 2005; Tang and Glassmaker 2010) both the moment and curvature at the adhesive zone tip are found to be zero,

$$M^*(0) = 0, \quad \frac{d^2\delta^*}{dx^{*2}}(0) = 0. \tag{12}$$

In the Supporting Material (Section S1) we present an alternative approach where the *vdW* attractions are not explicitly included in f^* but are accounted for at the adhesive zone tip by using nonzero curvature and moment conditions obtained from the j-integral. This approach represents the limit as the *vdW* decay length δ_c approaches zero. Physically it is less realistic but results in a simpler model. It is also explained in the Supporting Material (Section S1) that if all sources of adhesive attraction are considered explicitly in the adhesive stress f^* then the moment and curvature at the adhesive zone tip must be zero.

BCs far from the adhesive zone tip require more discussion. It is expected that, as the crack opening increases from the adhesive zone tip, the chains will undergo greater stretch and hence faster dissociation as indicated by Eq. (6); eventually the low bond density will cause f^* on the interface to be negligible. On the other hand, the decrease in force is continuous and f^* will approach but never actually reach zero. To resolve the dilemma of not having a clearly defined crack tip, we introduce the adhesive zone length L^*. Ideally this length would be defined so that $f^*(x^* = L^*)$ reduces below some tolerance; however, f^* can have a local minimum (data not shown), as the decay of the *vdW* portion can be stronger than the increase of the chain portion (stretching) for small openings. This local minimum makes such a criteria undesirable; therefore the following criteria was implemented

$$\Sigma_b^*(L^*) \leqslant \varepsilon_b^* \quad \text{and} \quad \delta^*(L^*) \geqslant \delta_{cr,vdW}^*. \tag{13}$$

Here the first condition ensures that at L^* the bond density and hence the adhesive stress from polymer chains has decreased below a desired tolerance. The second condition ensures that at L^* the crack has opened sufficiently far such that the work done by the *vdW* attractions is sufficiently close to the *vdW* work of adhesion. The critical *vdW* opening, $\delta_{cr,vdW}^*$, is a constant which depends on δ_c^*. If, for example, we require the work done by *vdW* attractions to be least 99% of W_{vdW}^* then $\delta_{cr,vdW}^* = 4.605\delta_c^*$. In the Supporting Material (Section S2) we explore a number of different criteria for determining L^* and found that the value of L^* can change considerably depending on what criteria is used. However, the fracture energies were found to be insensitive to the criteria. In light of the definition of L^* above, the traction outside of the adhesive zone is negligible. Therefore, from Eq. (9) the shear force must be constant and since only a moment, M_∞^*, is applied at the far field, the constant must be zero, i.e.

$$S^*(L^*) = 0. \tag{14}$$

Similarly, from Eq. (10), outside of the adhesive zone the moment must be constant and equal to the far field value, M_∞^*; therefore the necessary moment for crack propagation at a given speed V^* can be evaluated from $M_\infty^* = M^*(L^*)$.

2.4. Fracture Energies

Eqs. (6)–(14) constitute a boundary value problem that can be solved to compute the crack opening profile and adhesive zone length; however, a few additional steps are required to extract the energy release rate. The apparent energy release rate for crack growth, G^*, can be obtained from the work done by the applied moment to advance a unit area of the crack, after subtracting a strain energy correction due to the translating coordinate system (see Supporting Material, Section S3)

$$G^*(x^*) = \frac{M_\infty^*}{2} \frac{d^2\delta^*}{dx^{*2}}. \tag{15}$$

Eq. (15) is valid outside of the adhesive zone ($x^* > L^*$) where $S^* = 0$ and $M^* = M_\infty^*$, however G^* still depends on position because viscoelastic dissipation still occurs in the bulk material outside of the adhesive zone. The simple loading condition outside of the adhesive zone allows for an explicit expression for $d^2\delta^*/dx^{*2}$ to be derived from Eq. (8)

$$\frac{d^2\delta^*}{dx^{*2}} = \left(\left.\frac{d^2\delta^*}{dx^{*2}}\right|_{L^*} - \left.\frac{d^2\delta^*}{dx^{*2}}\right|_{\infty} \right) e^{-\frac{\gamma_E}{V^*}(x^* - L^*)} + \left.\frac{d^2\delta^*}{dx^{*2}}\right|_{\infty}. \tag{16}$$

Here $d^2\delta^*/dx^{*2}(L^*)$ is known from the solution within the adhesive zone. At infinity the beams are fully relaxed; therefore, $d^2\delta^*/dx^{*2}(\infty)$ can be evaluated by assuming the beam were elastic with the infinite time modulus

$$\left.\frac{d^2\delta^*}{dx^{*2}}\right|_{\infty} = \frac{M_\infty^*}{\gamma_E}. \tag{17}$$

Together with (16) and (17), the energy release rate can be evaluated from (15) at any given position x^* outside the adhesive zone.

The energy release rate as calculated above can also be expressed as

$$G^* = G_{ad}^* + G_{vis}^* \tag{18}$$

where G_{ad}^* is the work per unit area done by tractions within the adhesive zone, and G_{vis}^* is the viscous dissipation in the beam per unit area of crack advancement. G_{ad}^* can be calculated using the definition of work for a non-constant force

$$G_{ad}^* = \int_0^\infty f^* d\delta^* \approx \int_0^{\delta^*(L^*)} \Sigma_b^* F^* d\delta^* + W_{vdW}^*, \tag{19}$$

where we have separated the contributions to G_{ad}^* into components from polymer chains and *vdW* attractions. Since the traction is negligible outside of the adhesive zone the integration does not need to extend to δ greater than the crack opening displacement (COD),

$\delta^*(L^*)$. The viscous dissipation G^*_{vis} is obtained from Eq. (18) with G^* evaluated from Eq. (15) and G^*_{ad} evaluated from Eq. (19). Note that the energy of both beams' has been taken into account in the above equations.

3. Numerical methods

To solve Eqs. (6) and (8)–(10) a shooting method is used. First the value of $S^*(0)$ is guessed, which converts the boundary value problem into an initial value problem with initial conditions Eqs. (7), (11) and (12). A solution for $\{\Sigma_b{}^*(x^*)$, $S^*(x^*)$, $M^*(x^*)$, $\delta^*(x^*)$, $d\delta^*/dx^*$ and $d^2\delta^*/dx^*2\}$ is found by integrating Eq. (6) and (8)–(10) using a 4th order Runge–Kutta method with adaptive step size control (Press et al. 2007). $f^*(x^*)$ is calculated from Eq. (9) and the adhesive zone length L^* is determined from Eq. (13). After L^* is determined, the shear force at L^* is checked to satisfy Eq. (14). If it is not satisfied within some small tolerance, a new guess for $S^*(0)$ is made and the procedure repeats until Eq. (14) is satisfied.

The adhesive zone length can be sensitive to the criteria used in its definition (Eq. (13)), which was confirmed in the Supporting Material (Section S2) using results obtained from several different criteria. However G^*_{ad} was found to be the same for all criteria. This insensitivity allows us to present below the results obtained from a single criterion. The nontrivial results and discussion on L^* are given only in the Supporting Material (Section S4) so as not to distract from the main objectives of this work.

In addition, because bulk viscous dissipation within the beam can continue beyond the adhesive zone, the two energy release rates G^*_{vis} and G^* depend on the position x^* where they are evaluated and G^*_{vis} can greatly exceed the adhesive fracture energy if the beam length approaches infinity. Practically, it is more realistic to consider DCBs of finite length for evaluating these energies. We used several fixed beam lengths to compute the fracture energies, all of which are larger than the adhesive zone length. In Section 4 below we present representative results with a fixed beam length at $x^* = 1$ which is of the same order of magnitude as the largest adhesive zone length obtained with different combination of parameters used in this work. Other cases, including $x^* = \infty$, have been presented in the Supporting Material (Section S5).

4. Results and discussion

Even in the normalized form there are still seven parameters which govern the rate dependent fracture: V^*, γ_τ, γ_E, γ_L, U^*, W^*_{vdW} and δ^*_c. Among these, V^* and γ_τ can be identified as the most essential parameters since V^* is the normalized crack propagation speed while γ_τ captures the ratio of the relaxation times of the two sources of dissipation (bulk vs. interfacial). Therefore we vary V^* and γ_τ over many orders of magnitude (10^{-10} to 10^{10} for V^* and 10^{-5} to 10^3 for γ_τ), based on reported values of physical parameters (Chaudhury 1999; Ghatak et al. 2000; Hui et al. 2004). The remaining parameters are fixed at physically reasonable values. For γ_E, we will consider both an elastic case $\gamma_E = 1$, and a representative viscoelastic case where $\gamma_E = 0.01$ (Xu et al. 1992). The activation length λ has been reported as 0.1 nm (Evans and Ritchie 1997) for some biopolymers, and for $n = 150$ the contour length L_c has been reported to be 45 nm (Chaudhury 1999; Ghatak et al. 2000), thus a representative value of $\gamma_L = 0.02222$ will be used. A representative value of $U^* = 2850$ was found by numerically integrating experimental data from the work of Ghatak et al. (2000) to find U, and assuming standard ambient temperature and pressure (SATP) so that $T = 298$ K. Choosing a work of adhesion from dispersion forces of about $W_{vdW} = 50$ mJ/m^2 from Tang et al. (2007), and a bond density $\Sigma_o = 2.5 \times 10^{18}$ from Ghatak et al. (2000) gives, at SATP, $W^*_{vdW} = 5$. The *vdW* decay length is obtained from W^*_{vdW} and by assuming a *vdW* stress of about 2 MPa so that $\delta^*_c = 0.02$. In the Supporting Material, a sensitivity study for several values of δ^*_c is presented (Section S6).

With the above parameters, below we first study the rate-dependent fracture of an elastic DCB where bulk dissipation is absent (Section 4.1). This section is intended to elucidate the rate-dependent interfacial behavior before introducing the complexity of bulk viscoelastic behavior. In Section 4.2 we introduce bulk viscoelasticity in order to see the combined bulk and interfacial dissipation.

4.1. Elastic DCB

Consider the case of an elastic DCB, which can be obtained by setting $\gamma_E = 1$. This simplification removes viscous dissipation from the bulk. Therefore rate dependency will only come from interfacial bond dissociation. Studying this case will allow us to directly address the interfacial rate dependence so that later when we introduce bulk viscoelasticity it will be easier to identify the contributions from each rate-dependent process. Returning to Eq. (6) it is clear that the two parameters V^* and γ_τ can be grouped into a single parameter V^*/γ_τ. Also for the elastic DCB Eq. (8) can be replaced with $M^* = d^2\delta^*/dx^{*2}$; hence V^* and γ_τ do not appear individually in the formulation. Therefore, we will obtain results by varying V^*/γ_τ over a large range of values.

First consider Fig. 2(a) where the COD, $\delta^*(L^*)$, is shown on the y-axis and V^*/γ_τ is shown on the x–axis. At low V^*/γ_τ the crack opening is constant and there is no rate dependence. At high speed the COD appears to grow logarithmically. To understand these results, we note that when V^*/γ_τ is small the dissociation reaction, governed by Eq. (6), proceeds rapidly. Since the bonds dissociate so quickly the chains bridging the interface are not significantly stretched before the chain density becomes negligible. Hence, for small V^*/γ_τ the adhesive stress primarily comes from *vdW* attractions, represented by the last term in Eq. (9), which only depends on the crack opening and not on the rate of fracture. This is why there is no rate dependence at low speed as observed in Fig. 2(a), and the constant COD value at small V^*/γ_τ corresponds to the critical *vdW* opening $\delta^*_{cr,vdW} = 4.605\delta^*_c = 0.092$ for the parameters used here. At a critical V^*/γ_τ ($\approx$0.03 in Fig. 2(a)), the COD starts to exhibit rate dependent behavior. This transition occurs because the dissociation reaction in Eq. (6) slows down when V^*/γ_τ increases so that when the COD reaches the critical *vdW* opening there is still a considerable number of chains bridging the interface. As a result, the location of the crack tip is now determined by the kinetics of bond rupture for the polymer chains. Further increases in V^*/γ_τ result in even greater chain stretch, and therefore crack opening, before dissociation. This phenomenon causes the rate dependency seen in Fig. 2(a). It should be noted that until now we have only discussed how V^*/γ_τ in Eq. (6) affects bond dissociation; however it is important to understand that bond dissociation is coupled to the beams deflection through the exponential term in Eq. (6). While an increase in V^*/γ_τ slows down bond dissociation and allows for increased chain stretch, this stretch increases the tensile force on each chain and each bond therein, leading to an increase in the rate of bond dissociation. This feedback limits the increase of the COD to be logarithmic, as seen in Fig. 2(a).

Having noted that COD increases with V^*/γ_τ and greater COD implies that the chains have more stored energy, it is now of interest to consider the energy required to propagate a crack. For an elastic beam there is no bulk viscous dissipation so the only energy component is G^*_{ad} which is shown in Fig. 2(b) as a function of V^*/γ_τ; the embedded figure contains the same G^*_{ad} only plotted against the COD data from Fig. 2(a). As established during the discussion of Fig. 2(a), for slow crack propagation the fracture is governed by

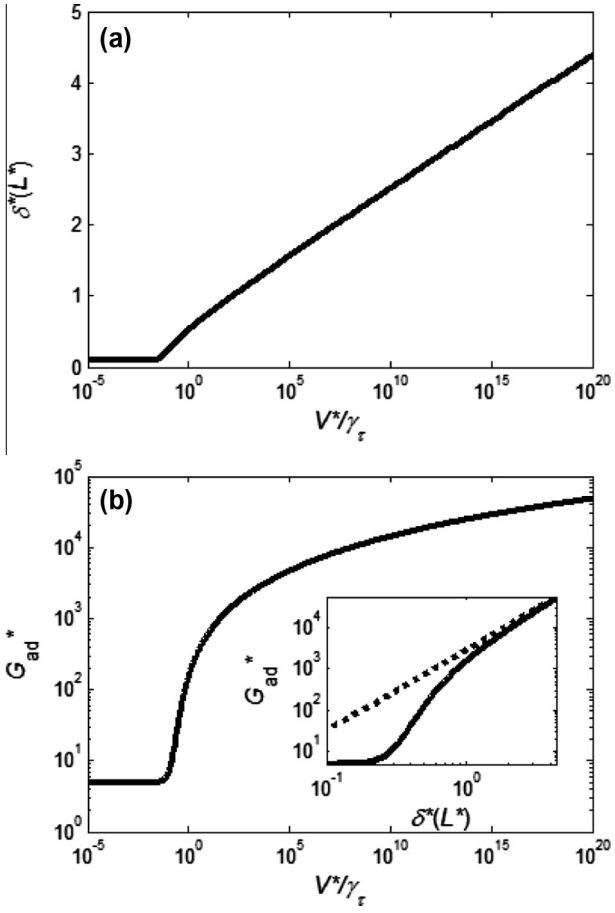

Fig. 2. Plots for (a) crack opening displacement, $\delta^*(L^*)$, and (b) adhesive fracture energy, G^*_{ad}, obtained by varying V^*/γ_τ while holding the other governing parameters fixed at $U^* = 2850$, $\gamma_E = 1$, $\gamma_L = 0.0022222$, $\delta_c{}^* = 0.02$ and $W^*_{vdW} = 5$. The embedded figure in (b) plots G^*_{ad} against the $\delta^*(L^*)$ result from (a) and the dotted line represents the analytical result based on a "reverse-step" distribution for the bond density.

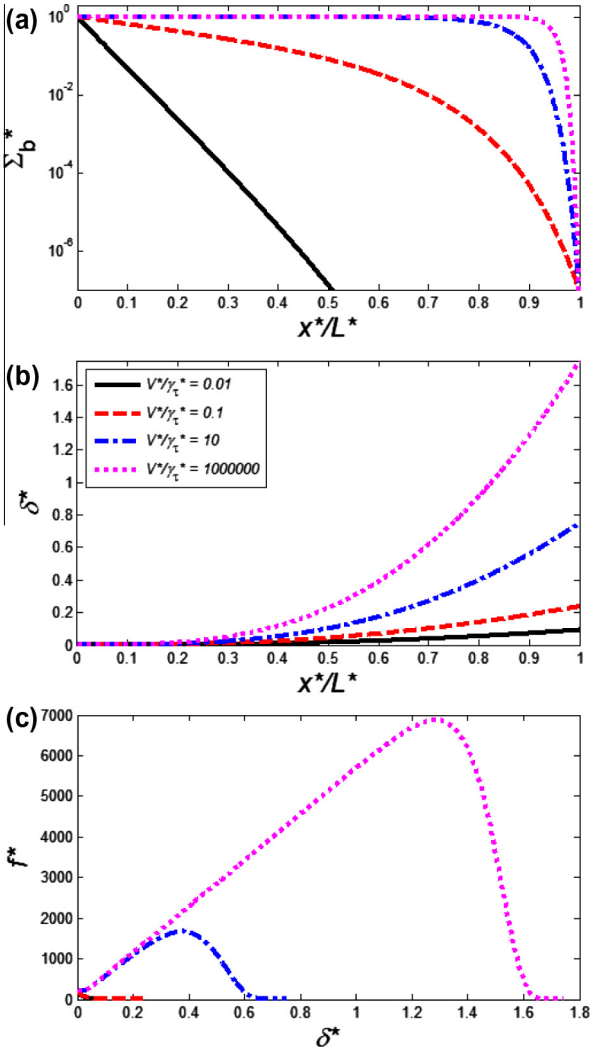

Fig. 3. Plots for (a) bond density Σ^*_b, (b) crack opening δ^* and (c) adhesive stress f^*. In each figure each curve represents a different value of V^*/γ_τ. Note that horizontal axis in (b) and (c) are x^*/L^*, where the adhesive zone length L^* for different curves would be different. Results were obtained while holding the following governing parameters fixed: $U^* = 2850$, $\gamma_E = 1$, $\gamma_L = 0.0022222$, $W^*_{vdW} = 5$ and $\delta_c = 0.02$.

the *vdW* attractions. The crack tip is located where the COD reaches the critical *vdW* opening, and within the adhesive zone the adhesive stress due to chain stretching is negligibly small. Hence, G^*_{ad} is equal to W^*_{vdW} at low speed, as shown in Fig. 2(b). As V^*/γ_τ is increased the rate of bond dissociation decreases and allows the chains, on average, to reach a greater stretch and store more energy before dissociating. Since all of the energy stored in the chains is lost when the bonds dissociate, the larger V^*/γ_τ causes G^*_{ad} to increase; physically this means that a greater moment M^*_∞ will be needed to propagate the crack. Although the energy dissipated by chains continuously increases as V^*/γ_τ is increased, G^*_{ad} remains approximately constant at W^*_{vdW} for $V^*/\gamma_\tau < 0.02$, which indicates that this energy needed to dissociate chain bonds remains negligible for a large range of slow crack propagation speeds.

It is of interest to study in detail how V^*/γ_τ impacts the bond density and adhesive stress within the adhesive zone, which is shown in Fig. 3. In Fig. 3(a), the bond density is shown in the *y*-axis and position relative to the adhesive zone tip is shown on the *x*-axis. Four curves are shown each for a different value of V^*/γ_τ. In all cases, the bond density starts at 1 and decreases with position. For the lowest V^*/γ_τ value (0.01), the bond density decays exponentially. As V^*/γ_τ is increased the distribution increasingly resembles a reverse step where all of the bonds remain unbroken until the edge of the adhesive zone where all bonds break at once.

To best understand this behavior it should be discussed in conjunction with Fig. 3(b) where the crack opening is plotted as a function of the position. In all cases the crack opening starts at zero and increases with position. Furthermore, at the same x^*/L^*, the magnitude of δ^* increases as V^*/γ_τ is increased. Consider the case of $V^*/\gamma_\tau = 0.01$. The crack opening in Fig. 3(b) is very small throughout the adhesive zone. As a result the exponential term in Eq. (6) is negligible, so the bond density is expected to decay exponentially which is confirmed in Fig. 3(a). Extending this idea, for any V^*/γ_τ, at the beginning of the adhesive zone the crack opening is small; thus initially the exponential term in Eq. (6) can be neglected. In a semilog plot, such as Fig. 3(a), the initial slope of the bond density curves should be $-\gamma_\tau/V^*$, and hence higher values of V^*/γ_τ have an initial slope closer to zero. Further from the adhesive zone tip where higher openings are reached, the chain stretch decreases the activation energy and accelerates the bond dissociation process. This acceleration is more significant for larger V^*/γ_τ. These two features, i.e., near zero initial slope and accelerated bond dissociation at higher openings, result in the bond density distribution approaching a reverse step distribution as V^*/γ_τ becomes large. In the extreme case of $V^*/\gamma_\tau \to \infty$, an exact reverse step

distribution is expected, and the same distribution exists for the so-called "rate independent" fracture (Hui et al. 2004), which was elucidated by considering the limit as the absolute temperature goes to zero. A consequence of the bond density distribution within the adhesive zone resembling a reverse step is that the adhesive stress, f^*, when plotted against the opening $\delta^*(x^*)$, will increasingly resemble a saw tooth as V^*/γ_τ becomes large. The adhesive stress vs. crack opening for different V^*/γ_τ can be seen in Fig. 3(c). At $\delta^* = 0$ the stress contributed by the chains is zero and the stress from *vdW* attractions is maximum. As the opening increases the *vdW* attractions decay, and each polymer chain is stretched so that the force F^* acting on it increases. The chain stress is $\Sigma_b^* F^*$, while the chain force F^* always increases with crack opening, the chain density Σ_b^* always decreases. This causes the adhesive stress to first increase with δ^* but eventually drop due to the rupture of polymer chain bonds.

Based on the above observations, an interesting result for G_{ad}^* can be obtained for the extreme case of $V^*/\gamma_\tau \to \infty$. In this limit, the bond density distribution is a reverse step function. Because the polymer chains remain intact within the adhesive zone, the distance over which the *vdW* stress is non-negligible is expected to be considerably smaller than the size of the adhesive zone. Therefore, as shown in the Supporting Material (Section S7), using the reverse step distribution for Σ_b^* and assuming $\delta_c^* = 0$ give a linear saw tooth distribution for the adhesive stress: $f^*(\delta^*) = 2U^*\delta^*$ up to $\delta^*(L^*)$. G_{ad}^* can then be derived in a closed form: $(G_{ad}^*)_{RS} = U^*[\delta^*(L^*)]^2 + W_{vdW}^*$ where $(G_{ad}^*)_{RS}$ is the adhesive fracture energy based on the reverse step bond density distribution. $(G_{ad}^*)_{RS}$ is plotted (dotted line) against the COD $\delta^*(L^*)$ in the embedded figure in Fig. 2(b). Clearly the results of G_{ad}^* converge to $(G_{ad}^*)_{RS}$ when V^*/γ_τ and hence $\delta^*(L^*)$ is large. The COD $\delta^*(L^*)$ in Fig. 2(a) shows logarithmic dependence on V^*/γ_τ at high speed, which can be written as $\delta^*(L^*) = \alpha \ln(\beta V^*/\gamma_\tau)$, α and β being constants. Introducing this results into $(G_{ad}^*)_{RS}$ gives the following expression

$$(G_{ad}^*)_{RS} = U^*[\alpha \ln(\beta V^*/\gamma_\tau)]^2 + W_{vdW}^*, \tag{20}$$

which is in agreement with the high speed dependency of G on V, $G \sim [\ln(V)]^2$, previously reported in the literature (Chaudhury 1999; Ghatak et al. 2000; Hui et al. 2004) for fracture in elastic medium with rate-dependent interfacial process.

4.2. Viscoelastic DCB

Now we consider results where bulk viscoelasticity is included by setting $\gamma_E = 0.01$. V^* is varied over a wide range of values and this process is repeated for five different values of γ_τ. As a complement to Fig. 2(a) we first plot the COD against V^*/γ_τ in Fig. 4. According to the normalization, Eq. (5), V^*/γ_τ is independent of the bulk relaxation time τ_o. The result is remarkably similar in behavior to Fig. 2(a), only this time there are different lines corresponding to different values of γ_τ, the ratio of bulk relaxation time over the characteristic time for chain dissociation. With this choice of x-axes, the curves for different γ_τ nearly collapse which suggests that γ_τ primarily functions as a speed shift in Eq. (6). Only minor differences can be observed for a limited range of V^*/γ_τ. This region has been enlarged in the embedded figure. The interfacial kinetics is coupled to beam deformation through the adhesive tractions from the polymer chains, yet compared with the elastic beam, Fig. 2(a), and over several orders of magnitude of γ_τ we observe only small differences. These differences are due to relaxation of the beams' effective modulus, and will be discussed later. Distributions of bond density and adhesive stress for a representative viscoelastic beam are shown in the Supporting Material (Section S8).

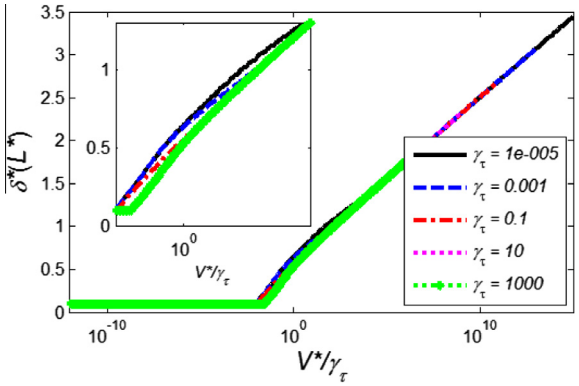

Fig. 4. Crack opening displacement, $\delta^*(L^*)$, plotted against V^*/γ_τ. This plot was obtained by varying V^* while keeping γ_τ fixed at the five values shown in the legend. The other governing parameters were held fixed at $U^* = 2850$, $\gamma_E = 1$, $\gamma_L = 0.0022222$, and $W_{vdW}^* = 5$. The embedded figure is zoomed in on the region around $V^*/\gamma_\tau = 1$ to better show details.

Although the influence of bulk viscoelasticity on COD appears to be minimal, when we consider the work needed to propagate the crack, G^*, bulk viscoelasticity is much more important. For a viscoelastic beam, there is dissipation within the beam which can increase for longer beams as mentioned previously. Here we have chosen to evaluate G^* at $x^* = 1$, which corresponds to a DCB with a fixed length that is larger than, but on the same order of magnitude as, the adhesive zone length L^*. In Fig. 5(a) the results for $G^*(1)$ are plotted against V^*/γ_τ. In the embedded figure the same $G^*(1)$ data is plotted against V^*. As in Fig. 4 each curve represents a different value of γ_τ. The main graph bears some resemblance to Fig. 2(b) but now the behavior is non-monotonic with each curve peaking at a different value of V^*/γ_τ. As Fig. 5(a) is not trivial to understand, we decompose G^* according to Eq. (18) and discuss the two components: G_{ad}^*, shown in Fig. 5(b), and G_{vis}^*, shown in Fig. 5(c).

Starting with Fig. 5(b), where G_{ad}^* is plotted on the y-axis and V^*/γ_τ is shown on the x-axis. In the embedded figure the same G_{ad}^* data is plotted against V^*. Unlike G^*, outside of the adhesive zone there will be no further contributions to G_{ad}^* so the result of G_{ad}^* is independent of the chosen beam length. First by comparing Fig. 5(a) and Fig. 5(b) the contribution from G_{ad}^* is significant. In addition, very much like the COD, not only does the behavior of G_{ad}^* closely resemble what was seen for the elastic case (Fig. 2b)), but all the curves corresponding to different γ_τ nearly collapse onto a master curve with only slight differences observed for a limited range of V^*/γ_τ. This implies that changing γ_τ primarily acts like an effective speed shift in the bond dissociation equation, Eq. (6). γ_τ does not appear in the beam equation, Eq. (8), and the fact that the speed is not shifted by γ_τ in the beam equation suggests that bulk viscoelasticity seems to have only a second-order impact on bond dissociation and the adhesive portion of the fracture energy. We will return to these second order effects, seen in Figs. 4 and 5 (b), after we examine the viscous portion of G^*.

Consider the portion of G^* from bulk viscous dissipation shown in Fig. 5(c). Here $G_{vis}^*(1)$ is shown on the y-axis, V^*/γ_τ is shown on the x-axis and each curve represents a different value of γ_τ. G_{vis}^* comes from the beam viscoelasticity, which is governed by Eq. (8) where γ_τ does not appear. Hence γ_τ does not directly impact the results of G_{vis}^*, and the normalized crack speed V^* would be a more suitable choice for the x-axis as shown in the inset of Fig. 5 (c). The behavior of $G_{vis}^*(1)$ is as follows. It approaches zero for both small and large V^*. Between these two limits there is a maximum, with the lowest values of γ_τ achieving the highest peak. These peaks are higher since V^*/γ_τ is larger and so is the associated crack

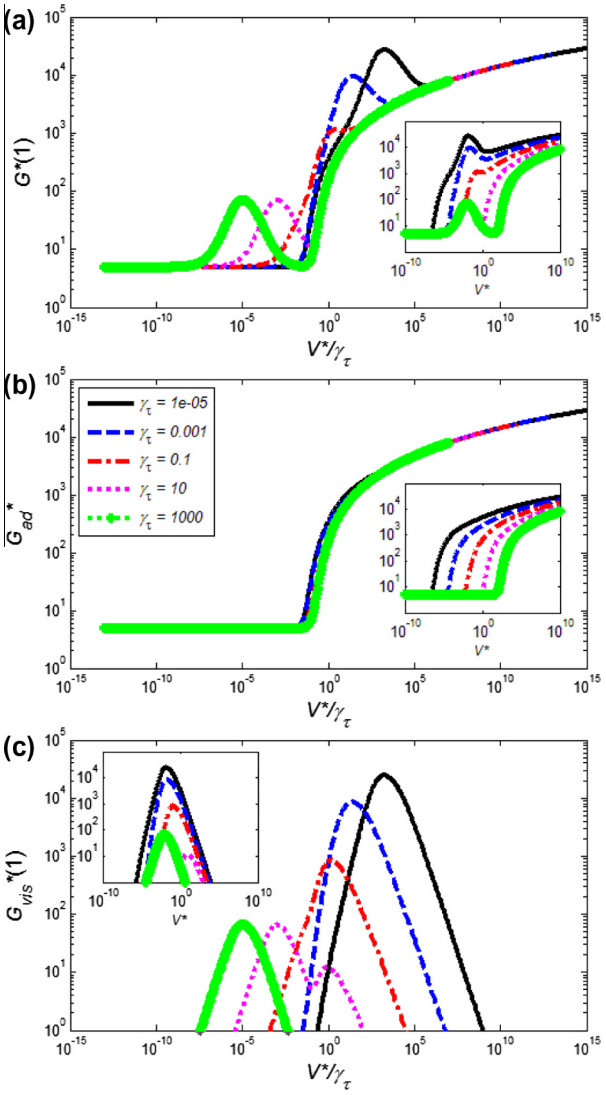

Fig. 5. Plots for (a) total fracture energy $G^*(1)$, (b) adhesive fracture energy G^*_{ad} and (c) viscous dissipation $G^*_{vis}(1)$, plotted against V^*/γ_τ. These plots were obtained by varying V^* while keeping γ_τ fixed at the five values shown in the legend. The other governing parameters were held fixed at $U^* = 2850$, $\gamma_E = 1$, $\gamma_L = 0.0022222$, and $W^*_{vdW} = 5$. Embedded figures shows the same data plotted against normalized crack propagation speed V^*.

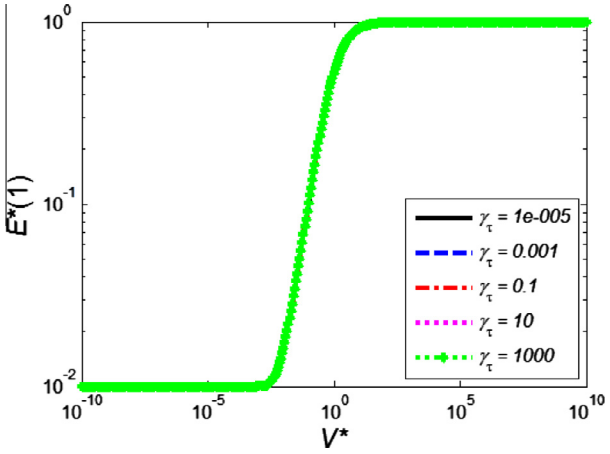

Fig. 6. Effective Young's modulus, $E^*(1)$, plotted against V^*. These plots were obtained by varying V^* while keeping γ_τ fixed at the five values shown in the legend. The other governing parameters were held fixed at $U^* = 2850$, $\gamma_E = 1$, $\gamma_L = 0.0022222$, and $W^*_{vdW} = 5$.

opening (Fig. 4) which results is greater deformation and hence dissipation. Comparing Fig. 5(c) and (a), it is clear that the peaks in Fig. 5(a) are caused by viscous dissipation.

To understand the viscous dissipation we make an analogy to an elastic beam and define a local effective modulus E^* so that $M^*(x^*) = E^*(x^*)d^2\delta^*/dx^{*2}$. Like G^* and G^*_{vis} the effective modulus varies with position so to compare with G^* (1) we have plotted $E^*(1)$ on the y-axis and V^* on the x-axis in Fig. 6(a). The behavior is simple: at low V^*, $E^*(1) = \gamma_E$, and as V^* is increased there is a transition to another plateau at high V^* where $E^*(1) = 1$. Physically this transition means that when the crack propagates slowly there is sufficient time for the beam to fully relax and the modulus decays to the infinite time value. When the crack propagates rapidly, within the fixed length under consideration, the beam has not yet had sufficient time to relax at all so the effective modulus is still the zero time modulus. Between these two extremes there is a viscoelastic transition. Comparing Figs. 6(a) and 5(c) it is clear that this transition occurs over the same speed range as the nonzero G^*_{vis}. To explain the behavior observed in Fig. 5(c), consider that as the beams deflect to open the crack they acquire strain energy from the work done by applied moments. However as the effective modulus of the beams relaxes, the strain energy stored in the beams is reduced even with a fixed deflection. This difference in strain energy is lost as viscous dissipation. At low speed negligible energy is lost because the beams relax to the infinite time modulus before there is any deflection or stored strain energy. Conversely at high crack propagation speed the beams deflect and have stored strain energy, however here the beams have not yet relaxed so viscous dissipation is again negligible. A consequence of this is that at high speed within the adhesive zone the beam is essentially elastic. Therefore, at very large V^*/γ_τ, G^*_{ad} and $G^*(1)$ approach $(G^*_{ad})_{RS}$ which was discussed earlier for the elastic beam and shown in the inset of Fig. 2(b).

Interestingly, for $\gamma_\tau = 10$ two peaks in $G^*_{vis}(1)$ can be seen in Fig. 5(c). The first peak can be attributed to the transition of E^* as discussed above. The second peak appears as V^* exceeds the critical value where the COD begins to increase above $\delta^*_{cr,vdW}$ (Fig. 4). The increased COD and beam deformation causes higher dissipation before eventually the unrelaxed limit shown in Fig. 6 is reached. This second increase in dissipation also results in the asymmetry visible for $\gamma_\tau = 0.1$ and 0.001 in Fig. 6(c).

One interesting observation made from Fig. 6 is that there is little difference between the $E^*(1)$ curves for different values of γ_τ. Pending a thorough explanation for this, we will use the E^* data in Fig. 6 to discuss the slight deviations between the curves for different γ_τ seen in Figs. 4 and 5(b). In Eq. (6) changing γ_τ is equivalent to a speed shift, however γ_τ does not appear in the beam equation (Eq. (8)). If we consider the actual speed V^* rather than the shifted speed V^*/γ_τ, as in the embedded figure in Fig. 5(b), at the same V^*/γ_τ we observe that curves for smaller γ_τ would be translated to lower speed. Since at lower V^* the effective modulus of the beam is smaller which lowers its flexural rigidity, the beam provides less resistance to crack opening. As a result, at the same V^*/γ_τ, for smaller γ_τ and hence smaller V^* the effective modulus is lower and therefore, the crack opening is slightly larger, as seen in Fig. 4. Since the chains have been stretched slightly more G^*_{ad} is also slightly larger as seen in the embedded figure of Fig. 5(b). In the Supporting Material (Section S9) we discuss the relaxation of E^* outside of the adhesive zone and the length of the dissipative zone relative to the adhesive zone.

So far we have qualitatively explained the results of our model and have taken several steps, either through literature comparison

(see Supporting Material Section S10) or by examining limits, to verify that a correct numerical solution to the governing equations has been obtained. Qualitatively our results match several other works in the literature. For example for a viscoelastic beam of fixed length it has been reported that G_{vis} is zero at high and low speed and has a critical speed where it is maximum (Xu et al. 1992), much like what was observed in Fig. 6(b). It has been experimentally observed that G increases with crack propagation speed (Gent 1996), and G_{ad} displays this same character (Fig. 5(b)). However, introducing coupled bulk and interfacial rate-dependence allows the model to explain or predict behavior not previously possible. For example, Figure 12 of (Ghatak et al. 2000) reported the rate dependency of fracture energy of silicone elastomers against an acrylic pressure-sensitive adhesive from rolling contact experiments. The fracture energy was shown to be significantly enhanced by introducing small amounts of H-bonding groups to increase the interfacial relaxation time without substantially increasing the surface energy. In addition, the fracture energy changed from nearly rate-independent to strongly rate-dependent upon the addition of H-bonding groups on the interface. In terms of our model the addition of H-bonding groups would be described by an increase in τ_-, which in turn leads to a decrease in γ_τ. Consulting the inset of Fig. 5(c) where the bulk viscous dissipation is plotted against the crack speed, asγ_τ decreases from 10 to 0.001, the peak $G^*_{vis}(1)$ value increases from approximately 60 to 8000; on a linear scale the former would appear rather rate insensitive in comparison to the latter case. This observation is qualitatively similar to the experimental observation of (Ghatak et al. 2000). Because our model has two characteristic time scales (one for bulk relaxation, and another for bond dissociation), an effective speed shift in G_{ad} can be created by varying the ratio of these two relaxation times. Furthermore, the coupling of bulk and interfacial rate dependence resulted in complex non-monotonic behaviors of G for finite sized beams (Fig. 5(a)). This behavior has the potential to offer much more flexibility in designing adhesive of a desired strength.

Often in viscoelastic fracture experiments the fracture energy G is expressed in the following form (Gent and Shultz 1972; Andrews and Kinloch 1973; Xu et al. 1992; Gent 1996; Ghatak et al. 2000; Rahulkumar et al. 2000)

$$G = W_o(1 + f(V)), \tag{21}$$

where W_o is the thermodynamic work of adhesion for separating the two surfaces under equilibrium conditions (Ghatak et al. 2000) (also referred to as the intrinsic strength (Andrews and Kinloch 1973)), and $f(V)$ represents the increase in fracture energy for finite rates of crack propagation. The function $f(V)$ has been described as the energy dissipated in the material at the propagating crack tip (Andrews and Kinloch 1973), the enhancement in strength when the adhesive is imperfectly elastic (Gent and Shultz 1972), or the energy expended in irreversible processes (Gent 1996). However it is not fully understood which physical processes this function represents (Gent 1996). It has been shown that the function depends not only on the micromechanical properties of the interface and viscoelastic properties of the bulk material but also on the specimen dimensions (Xu et al. 1992). In addition it has been proposed that the micromechanical properties of the interface must also be rate dependent (Rahulkumar et al. 2000), as is the case in the model presented in this work where interface kinetics are considered. To connect the results of our model to Eq. (21), we note that in our model as V approaches zero $W_o = W_{vdW}$. It then follows that $f(V) = (G - W_{vdW})/W_{vdW}$ which can be obtained by vertically shifting and scaling Fig. 5(a). The fact that $W_o = W_{vdW}$ as $V \to 0$ implies that to separate the two beams under equilibrium condition, one only needs to overcome the *vdW* attractions, while no energy is needed to break the polymer chains.

To explain this seemingly unrealistic result consider Eq. (6) where it can be seen that even if the force F^* on each chain is zero, the bond dissociation rate will be non-zero (i.e., the chain will break) unless the speed is very high. This implies that given enough time all bonds in the material would dissociate under zero load, which may be unphysical. This deficiency is directly due to the interfacial model we adopted in Eq. (6) which has been used in the literature several times (Chaudhury 1999; Ghatak et al. 2000; Hui et al. 2004). Rate equations have been written with the addition of a bond association term (Chaudhury 1999; Ghatak et al. 2000), however this term was assumed to be negligible. While it is true that bond association quickly becomes negligible as the crack opens, at low speed very small crack openings were observed and bond reforming can play an important role. Taking this into account can increase the bond density and G^*_{ad} at low speed.

To address another limitation of the present work, recall that the normalized crack opening was defined as $\delta^* = \delta/L_c$ where L_c is the contour length of the polymer chain. Given this definition physically within the adhesive zone we should have $0 \leqslant \delta^* \leqslant 1$. However, the COD was observed to be near 4.5 at high speed in Figs. 2(a) and 4. In other words, the model allows the crack to open too far at high speeds and this will over-predict G^*_{ad} in these cases. The source of this deficiency is likely the linearized force-extension relationship of the polymer chain as proposed in the literature (Chaudhury 1999; Ghatak et al. 2000). The notion of a nonlinear chain model has been explored (Ghatak et al. 2000; Hui et al. 2004). Tensile experiments on polymer chains show a force extension curve which is very flat for most of the extension but increases rapidly before the chain is fully stretched and fails (Ghatak et al. 2000). Taking into account this behavior should have two important effects on the model presented. First, the chain forces F^* at extensions near $\delta^* = 1$ would be much higher and through Eq. (6) would cause the chains to break before $\delta^* = 1$. Secondly, at low extensions the force acting on the chain would be much less, which combined with bond reforming would prevent the chain density from going to zero at small crack openings when the crack propagation speed is small.

Finally, it was observed that changing γ_τ over several orders of magnitude only created small changes in the effective modulus. A possible reason is the bulk viscoelastic beam model we have adopted. For a viscoelastic beam there is only one stress component and it is in the axial direction which is perpendicular to the direction of the extension of polymer chains. That is, there is no viscoelastic relaxation of the material in the direction of chain extension. Therefore, we expect that implementing higher dimensional continuum viscoelastic models could lead to stronger coupling between the bulk and interfacial rate processes and is a subject of future research.

5. Conclusion

In this work, the rate dependent fracture of a viscoelastic double cantilever beam (DCB) is studied. Two sources of rate dependence were considered. The beam itself was assumed to be a standard linear solid and an interfacial adhesion model describing the kinetics of breaking polymer chains was used. Within the adhesive zone, van der Waals (*vdW*) attractions were also considered. Seven nondimensional parameters governing the fracture of the DCB were identified, among which the impact of the V^* (normalized crack propagation speed) and γ_τ (ratio of bulk relaxation time to bond dissociation relaxation time) on the energy required to propagate the crack were discussed in detail. The apparent energy release rate G^* is made up of two components: the energy needed to overcome adhesion (G^*_{ad}), and viscous dissipation within the

bulk material (G^*_{vis}). G^*_{ad} increases with crack propagation speed, whereas G^*_{vis} is negligible for both small and large crack propagation speeds and has a maximum value at an intermediate V^*. The net result from the two dissipation mechanisms is that G^* varies non-monotonically with the crack propagation speed. A closed-form scaling relation between G^* and V^* was derived for very fast crack propagation. The relaxation time ratio γ_τ was shown to primarily function as a speed shift in affecting G^*_{ad}.

Acknowledgments

The authors acknowledge financial support from the Natural Science and Engineering Research Council (NSERC), Canada Foundation for Innovation, Alberta Innovates Technology Futures and the University of Alberta.

Appendix A. Supplementary data

Supplementary data associated with this article can be found, in the online version, at http://dx.doi.org/10.1016/j.ijsolstr.2015.08.020.

References

Anderson, T.L., 2005. Fracture Mechanics. CRC Press, Boca Raton.
Andrews, E.H., Kinloch, A.J., 1973. Proc. R. Soc. Lond. A 332, 385–399.
Chaudhury, M.K., 1999. J. Phys. Chem. B. 103, 6562–6566.
Chen, H., Feng, X., Huang, Y., Huang, Y., Rogers, J.A., 2013. J. Mech. Phys. Solids 61, 1737–1752.
Christiansen, R.M., 2003, . Theory of Viscoelasticity, second ed. Dover, New York.
Evans, E., Ritchie, K., 1997. Biophys. J. 72, 1541–1555.
Gao, X.-L., Su, Y.-Y., 2015. Acta Mech. http://dx.doi.org/10.1007/s00707-015-1357-8.
Gent, A.N., Shultz, J., 1972. Adhesion 3, 281–294.
Gent, A.N., 1996. Langmuir 12, 4492–4496.
Ghatak, A., Vorvolakos, K., She, H., Malotky, D.L., Chaudhury, M.K., 2000. J. Phys. Chem. B. 104, 4018–4030.
Glassmaker, N., Hui, C., 2004. J. Appl. Phys. 96, 3429–3434.
Hibbeler, R.C., 2005. Mechanics of Materials,, Pearson Prentice Hall, Singapore, pp 589, 607–614.
Hui, C.Y., Xu, D.B., Kramer, E.J., 1992. J. Appl. Phys. 72 (8), 3294–3304.
Hui, C.Y., Tang, T., Lin, Y.Y., Chaudhury, M.K., 2004. Langmuir 20, 6052–6064.
Kovalchick, C., Molinari, A., Ravichandran, G., 2014. ASME J. Appl. Mech. 2014 (81), 041016.
Lake, G.J., Thomas, A.G., 1967. Proc. R. Soc. London A 300 (1460), 108–119.
Press, W.H., Teukolsky, S.A., Vetterling, W.T., Flannery, B.T., 2007. Numerical Recipes The Art of Scientific Computing,, Cambridge University Press, Cambridge.
Rahulkumar, P., Jagota, A., Bennison, S.J., Saigal, S., 2000. Int. J. Soilds. Struct. 37, 1873–1897.
Rajagopal, K.R., Wineman, A., 1992. Int. J. Plasticity. 8, 385–395.
Rice, J.R., 1968. J. Appl. Mech. 35 (2), 379–386.
Tang, T., Jagota, A., Chaudhury, M., Hui, C.Y., 2007. J. Adhes. 87, 671–696.
Tang, T., Glassmaker, N., 2010. Math. Mech. Solids 15, 591–606.
Williams, M.L., Landel, R.F., Ferry, J.D., 1955. J. Am. Chem. Soc. 77 (14), 3701–3707.
Wineman, A., 2009. Int. J. Adv. Eng. Sci. Appl. Math. 1, 123–131.
Xu, D.B., Hui, C.Y., Kramer, E.J., 1992. J. Appl. Phys. 72 (8), 3305–3316.